2024 IEEE 22nd Mediterranean Electrotechnical Conference (MELECON) | 979-8-3503-8702-5/24/$31.00 ©2024 IEEE | DOI: 10.1109/MELECON56669.2024.10608778

Simulink-Based Simulation of Electric Bicycle Dynamics and Regenerative Braking for Battery State of Charge Assessment

Fabio Corti
DINFO
Università di Firenze
Firenze, Italy
fabio.corti@unifi.it

Marcello Minervini
Department of Engineering and Applied Sciences
University of Bergamo
Bergamo, Italy
marcello.minervini@unibg.it

Paolo Giangrande
Department of Engineering and Applied Sciences
University of Bergamo
Bergamo, Italy
paolo.giangrande@unibg.it

Alberto Reatti
DINFO
Università di Firenze
Firenze, Italy
alberto.reatti@unifi.it

Paolo Malighetti
Department of Management, Information and Production Engineering
University of Bergamo
Bergamo, Italy
paolo.malighetti@unibg.it

Luca Pugi
DIEF
Università di Firenze
Firenze, Italy
luca.pugi@unifi.it

***Abstract*—In this paper, a dynamic model for an e-bike is presented and its performance is evaluated. The model includes the main components constituting the vehicle electric drive such as the electric motor, the inverter, the DC-DC converter for speed control and regenerative braking, and the battery pack. The implementation is carried out in MATLAB-Simulink environment with the purpose of analyzing the power flows on the vehicle during target driving profiles. Unlike other models available in the literature, the developed model can represent a valuable tool to aid the designer in selecting and comparing different structural and component solutions. Knowing the efficiency of each component is possible to evaluate the global efficiency of the system in various operating conditions.**

Keywords—Micromobility, Simulation, Matlab, Simulink, E-Bike, Dynamic Model, Regenerative Braking, Sustainability.

I. Introduction

The growing importance of micromobility to mitigate the climate change and environmental degradation underscores the need for innovative solutions that reduce the ecological footprint of daily transportation. In this context, e-bikes represent a suitable solution for energy-efficient travel, reduce emissions, and enhance accessibility. Various barriers restrict the micromobility systems widespread and numerous multidisciplinary studies are ongoing for addressing the constraining challenges. In Table I, the most important topics currently under study are summarized [1]-[15].

A particularly important aspect lies in the management of charging infrastructure. Optimizing the number of charging stations in a specific area and strategically planning their locations based on users' primary routes play a key role and studies facing this subject are found in [1]-[4].

A crucial element of e-bikes is represented by the electric motor, which is capable of providing additional mechanical power to the user's pedalling in order to make commuting more enjoyable and less strenuous. In this perspective, significant efforts are focused on the development and optimization of electric motors featuring higher efficiency and improved power density. The goal of these efforts is therefore to optimize geometries and select the best materials to reduce size and costs while maintaining power output [5]-[15].

From an electrical point of view, the main elements constituting an e-bike power-train are shown in Fig. 1.

Regardless of the various available architectures, an e-bike is always characterized by an energy storage system, a power converter, and an electric motor. To minimize the weight of the bicycle, power converters required for recharging the battery are usually located within the charging infrastructure and are not integrated into the e-bike.

One of the significant advantages of using electric vehicles is the ability to perform regenerative braking. While many studies on this topic are available in the literature, they are primarily focused on electric car vehicles. Currently, there are few studies in the literature on regenerative braking in the field of micromobility due to the low kinetic energy available during braking (micromobility vehicles feature limited mass and reach contained speeds); some of them are resumed in Table I.

TABLE I. Micromobility Literature Overview

Issue	Reference
Infrastructure Management	[1], [2], [3], [4]
Electric Motor Design and Control	[5], [6], [7], [8], [9], [10], [11], [12]
Energy Management System	[13]
Battery Pack Design	[14], [15]

Authorized licensed use limited to: Universita degli Studi di Firenze. Downloaded on October 17,2024 at 16:09:17 UTC from IEEE Xplore. Restrictions apply.

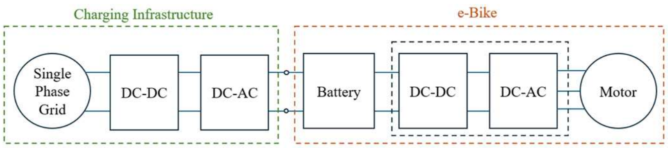

Fig. 1. Block diagram representation of an electric bycicle.

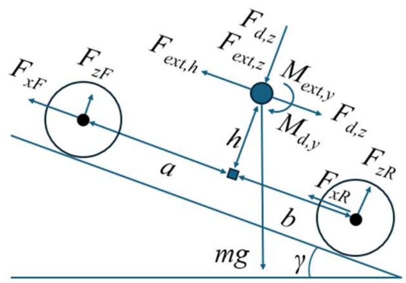

Fig. 2. Vehicle dynamic forces and moments.

As shown in [16]-[18], regenerative braking leads to significant energy storage only when the vehicle speed is not excessively low and when braking persists over time. Therefore, the control strategy should be capable to effectively evaluate whether performing regenerative braking or rely on mechanical braking, based on actual driving conditions. The same decision-making problem arises during the traction phase. Determining how much mechanical torque the electric motor should provide to assist the cyclist's pedaling falls within the decisions of the Energy Management System (EMS). Several studies have been proposed with the goal of optimizing user riding quality and maximizing energy stored in the batteries [13]. Finally, as shown in Table I, many studies are focused on optimizing energy storage. The target of these studies is to select the most suitable cell technologies for specific applications and optimize their quantity to ensure sufficient range to complete a given driving mission [14]-[15].

For this reason, to facilitate the improvement of all these aspects, an e-bike system-levels simulation tool is developed and built for enabling fast comparative analyses, which can quickly drive the decision process and the e-bike architecture evaluation. Furthermore, the simulation allows for the analysis of the vehicle's behavior under different driving profiles, namely varying speed and gradient profiles. This enables the selection of the best components for a specific mission and provides a preliminary idea of the appropriate sizing for the battery pack.

The paper is organized as follows. In Section II, the one dimension dynamic model of the e-bike is presented. In Section III, the model describing the torque provided by the cyclist is provided. In Section IV, the e-bike powertrain model is introduced. In Section V, the energy storage is described. In Section VI, the simulation results are presented while in Section VII, the conclusions are derived.

II. Vehicle Dynamic Model

One degree-of-freedom (1DOF) rigid vehicle body with constant mass undergoing longitudinal motion is used in this paper, as shown in Fig. 2. The choice of 1DOF model is due to its simplicity. It can provide a good approximation of the system's behavior without the added complexity of higher-dimensional models. In addition, simulating the dynamics of a system using 1DOF model is computationally less intensive compared to multi-dimensional models. This aspect is of primary importance when it is necessary to simulate driving missions that last hours. The mathematical model can be summarized by the following equations

$$F_b = m\ddot{x} \tag{1}$$

$$F_b = F_{xF} + F_{xR} - F_{d,x} + F_{ext,x} - mgsin\gamma \tag{2}$$

where F_b is the equivalent longitudinal force applied on the vehicle, m is the total mass and x is the longitudinal position of the vehicle. The equivalent force is made up of several contributions such as the longitudinal force on front wheel at the ground contact points F_{xF}, the longitudinal force on the rear wheel at the ground contact points F_{xR}, the longitudinal drag force on vehicle $F_{d,x}$, the external force along the vehicle-fixed x-axis (for example due to wind resistance) $F_{ext,x}$ and the force due to the slope of the road.

Zero normal acceleration and zero pitch torque determine the normal force on each front and rear axles.

$$F_{zF} = \frac{-M_{ext,y} - M_{d,y} + M_b - M_h}{N_F(a+b)} \tag{3}$$

$$F_{zR} = \frac{M_{ext,y} + M_{d,y} + M_a + M_h}{N_R(a+b)} \tag{4}$$

where $M_{ext,y}$ is the external moment about vehicle center of gravity (CG), $M_{d,y}$ is the torque due to drag on vehicle about the vehicle-fixed y-axis, N_F and N_R are the number of wheels on front and rear axle respectively and are assumed to be equal to one, since a bicycle is analyzed in this paper. The parameter a and b are the distance of front and rear axles, respectively, from the normal projection point of vehicle CG onto the common axle plane, respectively. Moreover the following moments are defined as $M_a=a(F_{d,z}+F_{ext,z}+mg\cos(\gamma))$, $M_b=b(F_{d,z}+F_{ext,z}+mg\cos(\gamma))$, $M_h=h(-F_{ext,x}+F_{d,x}+mg\sin(\gamma)+m\ddot{x})$. Finally, the wheel normal forces satisfy this equation

$$N_F F_{ZF} + N_R F_{ZR} - F_{ext,z} = mgcos(\gamma) \tag{5}$$

where $F_{ext,z}$ is the external forces applied to vehicle CG and it is assumed to be equal to zero. The equations used to calculate the drag force and moments acting on the vehicle are

$$F_{d,x} = \frac{1}{2TR} C_d A_f P_{abs} (\dot{x} - w_x)^2 \tag{6}$$

$$M_{d,y} = \frac{1}{2TR} C_{pm} A_f P_{abs} (\dot{x} - w_x)^2 (a+b) \tag{7}$$

where T is the ambient temperature, A_f is the frontal area, P_{abs} is the absolute pressure, $\dot{x}$ is the vehicle speed, w_x is the wind speed along the vehicle-fixed x-axis. The scheme resuming the main physical components is represented in Fig. 2.

The parameters used in the simulation are chosen standard and compatible value for an e-bike; e.g. the mass of the bike equal to 10 kg, speed of wind equal to 0, ambient temperature and pressure equal to 25°C, 1 atm.

Authorized licensed use limited to: Universita degli Studi di Firenze. Downloaded on October 17,2024 at 16:09:17 UTC from IEEE Xplore. Restrictions apply.

III. Cyclist Torque Model

The torque generated by the cycles is not constant and depends on the pedals position. In Fig. 3, the torque for different pedals angle position is shown. As first approximation, it is assumed that the driver is able to transfer its weight to the pedals during the motion [19]-[20]. Assuming that the driver has a weight of m_{driver}= 80 kg, and assuming a crank length of 175mm, the maximum torque is T_{driver}^{max} = 140 Nm.

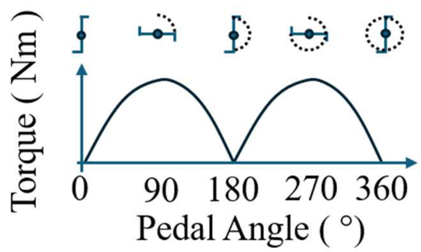

Fig. 3. Cyclist torque at different pedal angle.

Gears on bicycles serve to allow cyclists to adjust the effort required during pedaling based on the terrain and their physical resistance. Gears enable riders to change the relationship between pedaling and wheel rotation, allowing for more efficient cycling in different conditions. For instance, when tackling uphill sections, choosing a lower gear helps maintain a consistent cadence without exerting excessive muscle effort.

To simulate the gear shifting behavior, it was hypothesized to change the transmission ratio based on the longitudinal wheel speed, as shown in Fig. 4.

The torque generated by the driver, according to the speed can be therefore calculated as:

$$T_{driver} = \frac{T_{pedel}}{k_{trasm}} \tag{8}$$

IV. Electrical Drive

The position where electric motor is placed significantly influences the characteristics of the vehicle. Two main solutions are available: the hub motor and the mid-drive motor.

The hub motor is integrated directly into the wheel hub, making them relatively simple to install. The hub motors can be of type “geared” or “direct-drive”. The former has a planetary gear-box that increase the torque at bicycle low speed and reduce the weight of the motor. The latter is bulkier but can reach higher speed and produce less noise during operation. This integration simplifies the overall design of the electric bicycle. In addition, direct-drive hub motors support regenerative braking, since they don’t have internal free wheel mechanism,-allowing the electric bicycle to recover and store energy during braking. On the other hand, they may have limited torque, particularly when climbing steep hills. They may not provide as much assistance in challenging terrain compared to mid-drive motors.

Mid-drive motors generally provide better torque and efficiency compared to hub motors. They leverage the bicycle's gears, allowing for efficient power delivery and improved performance on hills.

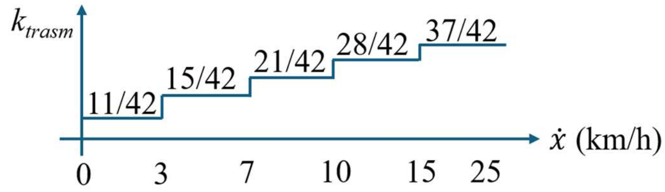

Fig. 4. Cyclist transmission ration k_{trasm} at difference bike speeds.

Mid-drive motors take advantage of the bike's existing gears, allowing for a more versatile and efficient power delivery. This is particularly beneficial in varied terrain. On the other hand, installing a mid-drive motor can be more complex and costly than a hub motor: a professional installation might be necessary. In addition, adopting this solution the regenerative braking is not possible due to rear derailleur and due to the freewheel in the rear wheel that don’t transmit the power backwards during decelerations.

A. Types of Motors

The two main types of electric motor actually used for e-bike applications are the Brushless DC Motor (BLDC) and the Brushless AC Motor (BLAC). The main difference in the construction of the two types of machine is the back electromotive force (*b.e.m.f.*). BLDC have a trapezoidal *b.e.m.f.*, while BLAC has a sinusoidal one. The factors that change the shape of the *b.e.m.f.* are the winding types, the span of the magnet over a pole, the pole and coil pitch, etc.

BLDC motors are relatively simple in design, which can result in lower manufacturing costs. They are widely available and have a mature technology base. This makes them easy to source and integrate into e-bike systems. In addition, BLDC motors can offer high power density, providing substantial power output for their size and weight. They need for a simple 120° resolution position sensor that is usually implemented through 3 Hall effect flux sensors. The main limitations of BLDC motors are their torque pulsations (especially at low speed) and limited torque at high speed.

BLAC motors generally offer high efficiency and good torque characteristics, especially at low speeds. This is advantageous for start-up and climbing hills. In addition, many BLAC motors can operate without position sensors (sensorless control), reducing complexity and potential points of failure. The main drawback concerns the position sensor higher cost compared to BLDC motors. In fact, the use of a resolver or an encoder is generally required for the sensored machines, which is more expensive than the 3-hall sensors used in BLDC. In addition, in some cases, BLAC motors may have slightly lower power density compared to BLDC motors, although advancements in motor design are continually addressing this [21].

B. Case Study

A three-phase direct-drive hub motor manufactured by nine continent (9C) is considered in the simulation (i.e., 9C+2707). The motor is equipped with rare-earth permanent magnets and each stator coil is formed by 7 turns. The rotor consists of 46 magnets with a width of 27 mm. The magnet thickness is about 3mm, while the length is about 13.5 mm.

Authorized licensed use limited to: Universita degli Studi di Firenze. Downloaded on October 17,2024 at 16:09:17 UTC from IEEE Xplore. Restrictions apply.

In Table II, the main characteristics of the motor, extrapolated from [22], are shown.

TABLE II. MOTOR MAIN CHARACTERISTICS

Parameter	Value
Actual Weight (kg)	6.1
Motor Power Range (W)	600
Magnetic Pole Pairs	23
Number of stator teeth	51
Motor Speed Constant (RPM/V)	9.1

In the context of the simulation, the control of the motor is assumed in closed-loop of the speed signal.

The torque-speed characteristics is shown in Fig. 5

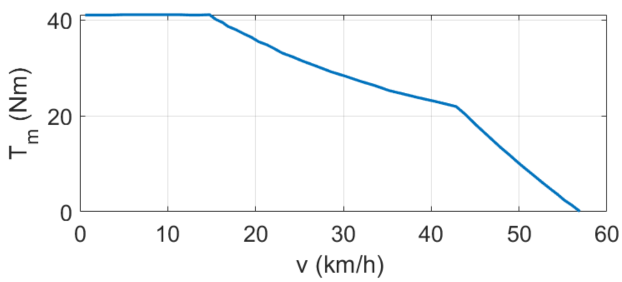

Fig. 5. Motor torque-speed characteristics.

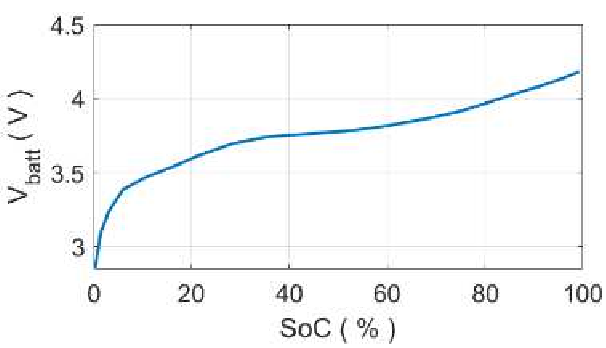

Fig. 6. Dependance of cell voltage V_{batt} from *SoC*.

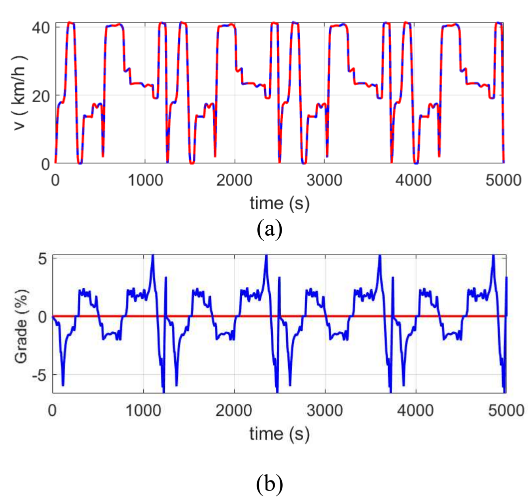

Fig. 7. Speed and grade profile. (a) Speed profile for Mission 1 and Mission 2. (b) Grade profile for Mission 1 (blue trace) and Mission 2 (red trace).

V. DC-DC CONVERTER MODELING

A bidirectional DC-DC converter is usually used as interface with the batteries for several reason. Firstly, during the traction phase, it is used to regulate the voltage at the input of the inverter. This allows to regulate the speed of the electric motor. Secondly, during the regenerative phase, the electric motor operates as a generator, converting kinetic energy back into electrical energy. The DC-DC converter can boost the electromagnetic force generated on the motor to properly charge the battery.

Although the DC-DC converter is modelled via a constant efficiency ($\eta_{DC\text{-}DC}$=0.9) for the sake of fast simulation time, more detailed DC-DC converter modelling approach could have been employed [23].

VI. ENERGY STORAGE SYSTEM: LI-ION BATTERY PACK

In micromobility, the most common energy storage technology is represented by the Li-Ion batteries [25]-[26]. After some analysis, a battery pack made up by two parallel of ten Samsung INR21700-48X cells connected in series have been chosen (for a rated voltage of 36 V). The main characteristics are summarized in Table III. As first approximation, the voltage vs SoC dependence shown in Fig. 6 has been assumed.

TABLE III. BATTERY PACK CHARACTERISTICS

Parameter	Value
Rated Voltage	3.6 V
Max/Min Voltage	4.2V / 2.5 V
Capacity	4.8 Ah
Maximum Discharge Current	9.6 A

VII. DRIVE CYCLES

In order to evaluate the effects of the mission profile on the regenerative braking, the two different drive cycles shown in Fig. 7 have been tested. The blue trace is referred as mission profile M1, while the red trace is referred as mission profile M2. Both the missions have the same speed profile, as shown in Fig. 7(a). The difference between the two profiles is the slope of the track. For the first mission profile (M1), the slope of the track is assumed to be equal to always zero, as shown in Fig. 7(b).

The results are shown in Fig. 8(a) and (b), where the four translational forces acting on the vehicle during the mission profile M1 and M2 respectively are shown. The forces that produce positive acceleration are the force delivered by the rider $F_{Cyclist}$ and the force generated by the electric motor during the pulling phase F_m. On the other hand, the forces that produce deceleration are the force from the mechanical brakes F_{mech} and the force produced by the electric motor during regenerative braking F_r. In Fig. 9, the current flowing through the battery and the SoC for the profile M1 with regenerative braking is shown.

The comparison in terms of final SoC for the four cases are summarized in Table IV. The results show that allowing the regenerative braking, it is possible to recover up to 4.7 %. As expected, energy recovery is more pronounced for those stretches characterized by profiles that allow non-instantaneous

Authorized licensed use limited to: Universita degli Studi di Firenze. Downloaded on October 17,2024 at 16:09:17 UTC from IEEE Xplore. Restrictions apply.

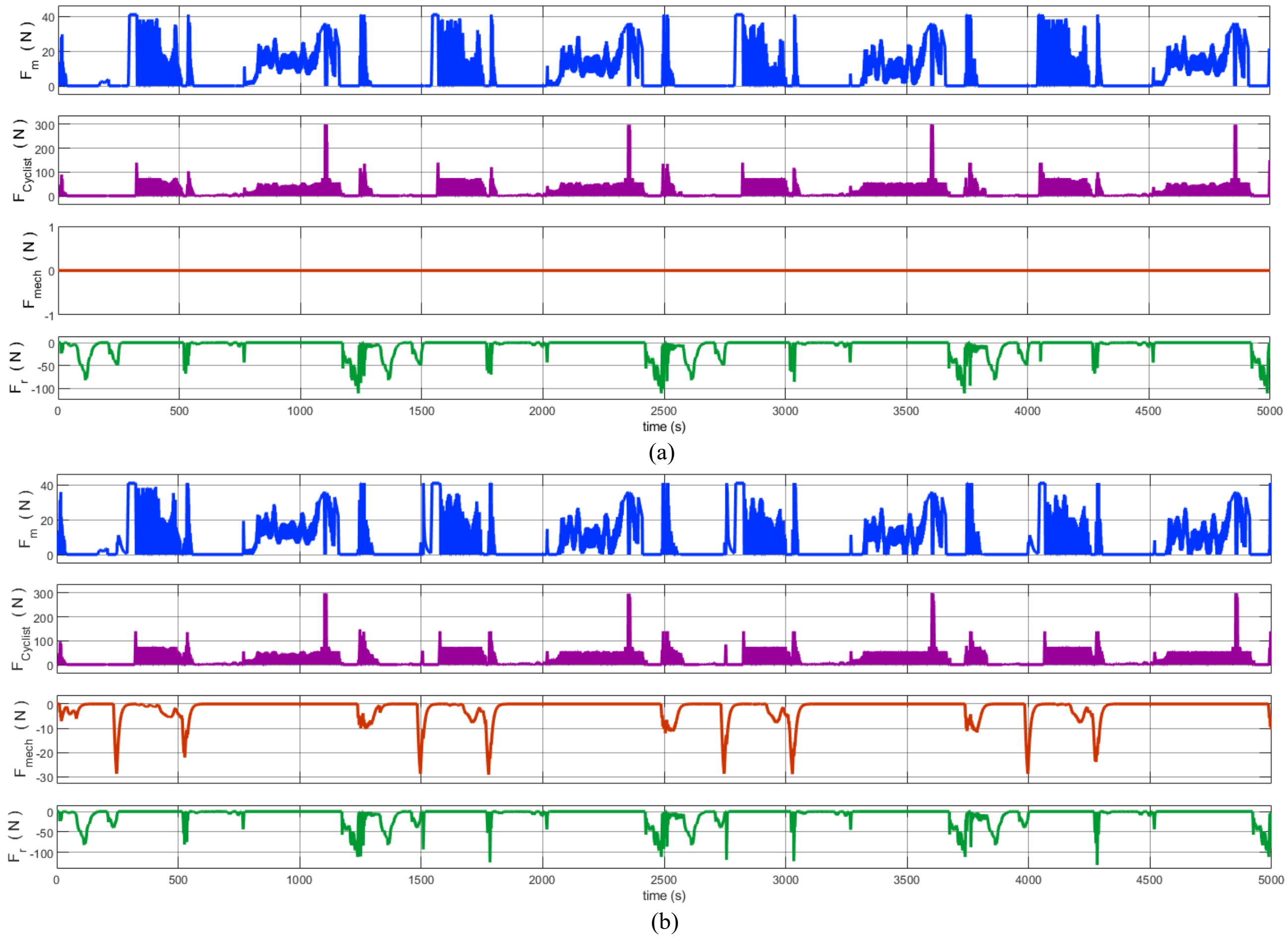

Fig. 8. Traslational forces acting on the bycicle. (a) Mission profile 1. (b) Mission profile 2.

but prolonged braking at not excessively high speeds. Therefore, the extent of benefit in using regenerative braking system is closely related to the mission to be solved. This Simulink model is meant to facilitate the evaluation process at a preliminary stage of e-bike design.

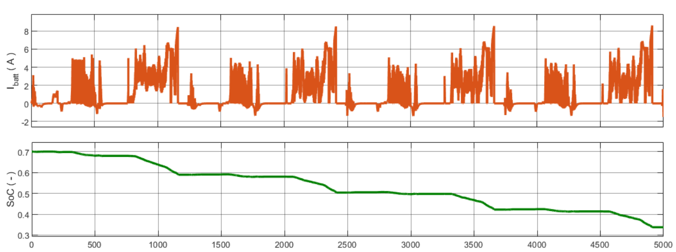

Fig. 9. Current flowing through the battery (red trace) and State of Charge during the misssion profile M1 with regenerative braking.

TABLE IV. SIMULATION RESULTS: FINAL SOC

Case Study			Value	Extended Range
Final SoC	Profile 1	No Regen. Braking	29.1 %	+ 4.7 %
		Regenerative Braking	33.8 %	
	Profile 2	No Regen. Braking	16.9 %	+ 2 %
		Regenerative Braking	18.9 %	

VIII. CONCLUSIONS

In this paper, a Simulink model able to model the dynamic of an e-bike was built. The developed model takes into account the main components of the e-bike powertrain including the regenerative braking feature. Key strengths of the system-level simulation tool are its user-friendly nature and the light calculation burden, which enable fast comparison among different electric drive components and mission profiles orienting the preliminary design choices. Considering the investigated e-bike architecture, the regenerative braking allows to achieve a driving range extension of 4.7% when a flat mission profile is simulated, while the same value is reduced to 2% in case of sloped road. In the latter case, a greater amount of energy is recovered although more power is drained from the battery, since the rider power is kept constant and the mission

Authorized licensed use limited to: Universita degli Studi di Firenze. Downloaded on October 17,2024 at 16:09:17 UTC from IEEE Xplore. Restrictions apply.

profile is more challenging due to the climbing sections of the mission profile.

ACKNOWLEDGMENT

This study was also carried out within the MOST {Sustainable Mobility National Research Center} and received funding from the European Union Next-GenerationEU (PIANO NAZIONALE DI RIPRESA E RESILIENZA (PNRR) {MISSIONE 4 COMPONENTE 2, INVESTIMENTO 1.4} D.D. 1033 17/06/2022, CN00000023), Spoke 5 \"Light Vehicle and Active Mobility". This manuscript reflects only the authors' views and opinions, neither the European Union nor the European Commission can be considered responsible for them.

REFERENCES

[1] N. Schelte, H. Straßberger, S. Severengiz, S. Finke and B. Felmingham, "Environmental Impact of Off-grid Solar Charging Stations for Urban Micromobility Services," *2021 IEEE European Technology and Engineering Management Summit (E-TEMS)*, Dortmund, Germany, 2021, pp. 33-39.

[2] A. Duz and M. Corno, "Flexible Pricing Strategies in Electric Free-Floating Bicycle Sharing," in *IEEE Access*, vol. 9, pp. 152972-152983, 2021, doi: 10.1109/ACCESS.2021.3127568.

[3] P. Zhong, A. Xu, Y. Chen, F. Gao and G. Duan, "An Optimization Deployment Scheme for Static Charging Piles Based on Dynamic of Shared E-Bikes," *2019 15th International Conference on Mobile Ad-Hoc and Sensor Networks (MSN)*, Shenzhen, China, 2019, pp. 343-347, doi: 10.1109/MSN48538.2019.00071.

[4] E. Collini, P. Nesi and G. Pantaleo, "Deep Learning for Short-Term Prediction of Available Bikes on Bike-Sharing Stations," in *IEEE Access*, vol. 9, pp. 124337-124347, 2021.

[5] R. Nasiri-Zarandi, A. Karami-Shahnani, M. S. Toulabi and A. Tessarolo, "Design and Experimental Performance Assessment of an Outer Rotor PM-Assisted SynRM for the Electric Bike Propulsion," in *IEEE Transactions on Transportation Electrification*, vol. 9, no. 1, pp. 727-736, March 2023.

[6] J. Lin, N. Schofield and A. Emadi, "External-Rotor 6−10 Switched Reluctance Motor for an Electric Bicycle," in *IEEE Transactions on Transportation Electrification*, vol. 1, no. 4, pp. 348-356, Dec. 2015, doi: 10.1109/TTE.2015.2502543.

[7] Y. Yang, M. M. Rahman, T. Lambert, B. Bilgin and A. Emadi, "Development of an External Rotor V-Shape Permanent Magnet Machine for E-Bike Application," in *IEEE Transactions on Energy Conversion*, vol. 33, no. 4, pp. 1650-1658, Dec. 2018.

[8] T. -A. Huynh, V. -H. Che and M. -F. Hsieh, "Maximization of High-Efficiency Operating Range of Spoke-Type PM E-Bike Motor by Optimization Through New Motor Constant," in *IEEE Transactions on Industry Applications*, vol. 59, no. 2, pp. 1328-1339, March-April 2023, doi: 10.1109/TIA.2022.3205571.

[9] B. Howey, B. Bilgin and A. Emadi, "Design of an External-Rotor Direct Drive E-Bike Switched Reluctance Motor," in *IEEE Transactions on Vehicular Technology*, vol. 69, no. 3, pp. 2552-2562, March 2020, doi: 10.1109/TVT.2020.2965943.

[10] N. Tadrist and H. Zeroug, "Sensorless Control with Back EMF Integration Method for E-bike," *2022 International Conference of Advanced Technology in Electronic and Electrical Engineering (ICATEEE)*, M'sila, Algeria, 2022, pp. 1-6.

[11] A. Dash, "Hybrid Control Algorithm for BLDC Drive Involving Battery and Supercapacitor in E-bikes," *2022 International Virtual Conference on Power Engineering Computing and Control: Developments in Electric Vehicles and Energy Sector for Sustainable Future (PECCON)*,, India, 2022, pp. 1-6.

[12] H. Purnata, M. Yusuf and S. D. Riyanto, "Closed Loop System BLDC Motor For Electric-Bike," *2020 International Conference on Applied Science and Technology (iCAST)*, Padang, Indonesia, 2020, pp. 422-428, doi: 10.1109/iCAST51016.2020.9557642.

[13] M. Corno, A. Duz and S. M. Savaresi, "Design of a Charge-Sustaining Energy Management System for a Free-Floating Electric Shared Bicycle," in *IEEE Transactions on Control Systems Technology*, vol. 30, no. 2, pp. 654-666, March 2022.

[14] M. Laschi *et al*., "Simulation-based assessment of Supercapacitors as Enabling Technology for Fast Charging in Micromobility," *2022 IEEE 21st Mediterranean Electrotechnical Conference (MELECON)*, Palermo, Italy, 2022, pp. 890-895.

[15] Gangchul Kim, Chongpyo Cho, Youngdug Pyo and Wookhyun Lee, "The development of stand-alone battery pack for micro mobility EV," *2016 IEEE Transportation Electrification Conference and Expo, Asia-Pacific (ITEC Asia-Pacific)*, Busan, Korea (South), 2016, pp. 874-876.

[16] P. Fajri, S. Lee, V. A. K. Prabhala and M. Ferdowsi, "Modeling and Integration of Electric Vehicle Regenerative and Friction Braking for Motor/Dynamometer Test Bench Emulation," in *IEEE Transactions on Vehicular Technology*, vol. 65, no. 6, pp. 4264-4273, June 2016, doi: 10.1109/TVT.2015.2504363.

[17] S. Heydari, "Maximizing Regenerative Braking Energy Recovery of Electric Vehicles Through Dynamic Low-Speed Cutoff Point Detection," in *IEEE Transactions on Transportation Electrification*, vol. 5, no. 1, pp. 262-270, March 2019.

[18] X. Nian, F. Peng and H. Zhang, "Regenerative Braking System of Electric Vehicle Driven by Brushless DC Motor," in *IEEE Transactions on Industrial Electronics*, vol. 61, no. 10, pp. 5798-5808, Oct. 2014, doi: 10.1109/TIE.2014.2300059.

[19] M. Schmitt, S. Decker, L. Leister, A. Liske and M. Doppelbauer, "Measuring and Characterization of a Pedal Electric Cycle (Pedelec) Drivetrain on a Test-Bench for Modelling and Optimization," *2021 IEEE Vehicle Power and Propulsion Conference (VPPC)*, Gijon, Spain, 2021, pp. 1-6.

[20] M. Schmitt, S. Decker and M. Doppelbauer, "Measuring and Characterization of a Pedal Electric Cycle (Pedelec) on a Full System Test-Bench with Full Range Emulation of a Cyclist," *2019 21st European Conference on Power Electronics and Applications (EPE '19 ECCE Europe)*, Genova, Italy, 2019, pp. P.1-P.10, doi: 10.23919/EPE.2019.8915567.

[21] Contò C, Bianchi N. E-Bike Motor Drive: A Review of Configurations and Capabilities. *Energies*. 2023; 16(1):160.

[22] https://ebikes.ca/tools/simulator.html [accessed January 2024]

[23] S. S. Sayed and A. M. Massoud, "Review on State-of-the-Art Unidirectional Non-Isolated Power Factor Correction Converters for Short-/Long-Distance Electric Vehicles," in *IEEE Access*, vol. 10, pp. 11308-11340, 2022.

[24] G. -J. Chiou, Y. -K. Tang, J. -Y. Chen and C. -S. Hsu, "Implementation of Phase Shift Full-Bridge Converter Using GaN FET for EV Charger," *2021 IEEE International Future Energy Electronics Conference (IFEEC)*, Taipei, Taiwan, 2021, pp. 1-6, doi: 10.1109/IFEEC53238.2021.9661790.

[25] C. -L. Nguyen, P. Primiani, L. Viglione and L. Woodward, "A Low-Cost Battery Charger Usable with Sinusoidal Ripple-Current and Pulse Charging Algorithms for E-Bike Applications," *2019 IEEE 28th International Symposium on Industrial Electronics (ISIE)*, Vancouver, BC, Canada, 2019, pp. 2085-2090, doi: 10.1109/ISIE.2019.8781248.

[26] A. Dash, A. K. Sahu, S. Sharma, D. Yadav, M. Fuad and S. Chatterjee, "Design and Analysis of Electric Bike(E-Bike)," *2023 2nd International Conference on Smart Technologies and Systems for Next Generation Computing (ICSTSN)*, Villupuram, India, 2023, pp. 1-7, doi: 10.1109/ICSTSN57873.2023.10151644.

[27] M. Savrum and G. Poyrazoglu, "Safety Test Setup Installation for E-bike Battery Systems," *2022 4th Global Power, Energy and Communication Conference (GPECOM)*, Nevsehir, Turkey, 2022, pp. 139-144, doi: 10.1109/GPECOM55404.2022.9815788.

Authorized licensed use limited to: Universita degli Studi di Firenze. Downloaded on October 17,2024 at 16:09:17 UTC from IEEE Xplore. Restrictions apply.